

Not Ions Alone: Barriers to Ion Permeation in Nanopores and Channels

Oliver Beckstein, Kaihsu Tai, and Mark S. P. Sansom*

Department of Biochemistry, University of Oxford, South Parks Road, Oxford OX1 3QU, UK

Received August 5, 2004; E-mail: mark@biop.ox.ac.uk

Confinement at the molecular scale strongly affects the behavior of water and ions and can lead to effects that are not anticipated from macroscopic descriptions.^{1–7} One example is the exclusion of ions from pores that have radii much larger than the ionic radius.⁸ Pores of molecular dimensions (radius $R \leq 1$ nm) can be found, for instance, in carbon nanotubes, zeolites, and ion channel proteins. We show that an electrostatic continuum approach alone does not capture the essentials of ion permeation through pores in a low dielectric. A more detailed atomistic approach is required that incorporates both the interaction of the water molecules with the ion (the hydration shell) and the water–pore interaction (hydrophobic effects).

Earlier atomistic molecular dynamics (MD) simulations⁸ indicated that short (length $L = 0.8$ nm) model nanopores with a methyl-terminated surface would not allow the passage of ions below a critical radius $R \leq 0.6$ nm. Such narrow “hydrophobic” pores are believed to form the gates in some ion channels.^{10–13} Different effects must play a role in creating a barrier to ion permeation. For any charged species there is a purely electrostatic “dielectric barrier”¹⁴ to transferring an ion from a high dielectric phase like water through a low dielectric membrane, generally referred to as the Born energy.¹⁵ An atomistic picture includes the interaction between individual water molecules and the solute and the entropic cost of accommodating the solute cavity. The energetic cost for stripping the hydration shell off an ion is the free energy of solvation. In the context of channel gating, it was hypothesized that ion dehydration would create a barrier to ion permeation.^{10,16–18}

To address this hypothesis we look at the behavior of ions and water in radically simplified pore models.⁸ A pore consists of two mouth regions (length 0.4 nm and radius 1.0 nm) at either end of the constriction site of length $L = 0.8$ nm and varying radii $0.15 \text{ nm} \leq R \leq 1.0$ nm. The pore is hydrophobic with the characteristics of a methyl-terminated surface and is embedded in a membrane mimetic of the same material (inset of Figure 1). We quantify the observed exclusion of ions (and water) from hydrophobic pores in terms of their free energy permeation barrier ΔG^\ddagger . It is the maximum of the equilibrium free energy landscape as described by the one-dimensional potential of mean force^{19,20} (PMF) $\Delta G(z)$, i.e., the free energy required to position a particle at subsequent positions z along the pore axis.

First we turn to the continuum picture (Figure 1). One limiting case is the barrier to permeation through a low dielectric slab without a pore. The Poisson–Boltzmann calculation yields a barrier of 135 kT (at $T = 300\text{K}$, 336 kJ mol^{-1}), about 81% of the hydration energy of the sodium ion.¹⁵ This large energetic cost is considerably lowered by translocating through an aqueous pore. For a radius of $R = 0.55$ nm, ΔG_B^\ddagger drops to 0.23 kT , i.e., the barrier effectively vanishes. Only for $R \leq 0.4$ nm it drops below 1 kT , ceasing to be a barrier for all practical purposes. This is in stark contrast to the results from the atomistic MD simulations (Figure 2), which indicate that in the wide $R = 0.55$ nm pore an ion still has to overcome a

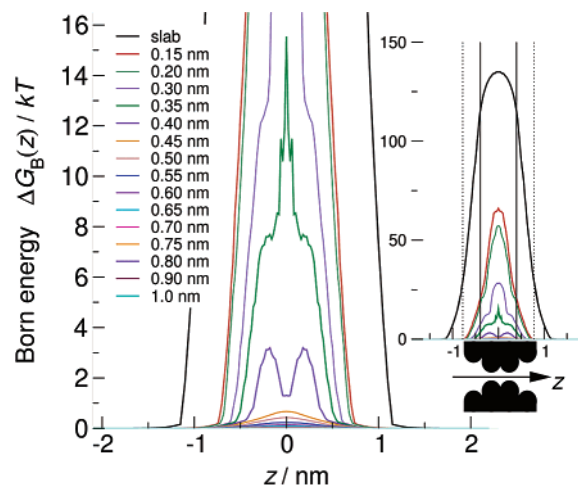


Figure 1. Born energy profiles $\Delta G_B(z)$ from the continuum electrostatic calculations. $\Delta G_B(z)$ is the Born energy at z , obtained by solving the Poisson–Boltzmann equation (using the APBS package;⁹ see Supporting Information for details). Dotted vertical lines in the inset denote the surface of the slab, while continuous lines denote the extent of the pore with $L = 0.8$ nm, as shown in the schematic.

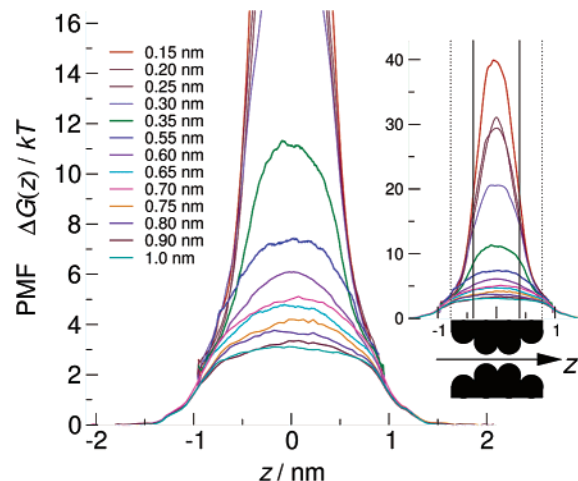


Figure 2. Atomistic PMF profile $\Delta G(z)$ for ion permeation through pores with various radii. $\Delta G(z)$ is calculated from classical MD trajectories using the GROMACS package.²¹ For wider pores ($R \geq 0.65$ nm), 100 ns equilibrium MD yielded a converged density, and so $\Delta G(z) = -\ln(z)/n_0$. For $R \leq 0.65$ nm, umbrella sampling²² with the WHAM unbiasing procedure²³ was employed (see the Supporting Information).

barrier of 7.4 kT , and even a pore with a diameter of 2 nm (more than the total thickness of the slab) will have an appreciable effect on ion permeation ($\Delta G^\ddagger = 3.2 \text{ kT}$).

Figure 3 compares the barrier heights obtained from the two different approaches. The failure of the continuum model to describe the PMF in narrow pores is not unexpected and has been noted before.²⁴ It is somewhat more surprising in the wider pores (about

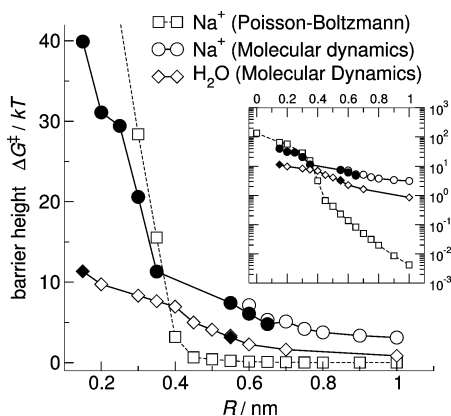


Figure 3. Comparison of the barrier height ΔG^\ddagger from the electrostatic $\Delta G_B(z)$ and atomistic $\Delta G(z)$ PMF profiles. Data points indicated by filled circles or diamonds were calculated from umbrella-sampled MD trajectories, whereas the empty variants were directly obtained from equilibrium MD. Empty squares were obtained from continuum-electrostatic Poisson–Boltzmann calculations.

$R \geq 0.6$ nm) where a continuum description of the solvent electrolyte should become feasible. Investigation of the ionic density in the pore nevertheless shows a 0.6 nm depletion layer near the surface and a density in the $R = 1$ nm pore barely reaching 70% of the bulk value. Atomistic simulations include entropic and short-range interaction effects in addition to long-range electrostatics, and they also account for the granularity of the solvent, thus allowing for density effects. The situation in the narrow pores ($R \leq 0.3$ nm) can be interpreted in both pictures in a qualitatively similar way. The pore is too narrow to accommodate solvent together with the ion. In the Born picture, this corresponds to an ion completely immersed in a low dielectric environment. The atomistic picture describes it as the loss of the hydration shell (perhaps apart from two water molecules in axial positions, which can still contribute up to half of the total solvation energy²⁵). In both cases, this translates into a high energy barrier. For $R \geq 0.4$ nm, the ion is enveloped by a shell of high dielectric solvent at least 0.1 nm thick. This is already enough to lower the Born energy considerably. The continuum calculations assume that the solvent simply exists in the pore. There is no energetic cost associated with filling the pore with water. The PMF for water shows that the free energy to place a water molecule at the center of the pore is considerable (between $3kT$ and $7kT$ for medium-sized pores, see Figure 3). This means it is difficult to maintain a solvent environment in the pore that in turn could successfully hydrate and stabilize the ion (although collective effects will reduce the barrier to filling the pore with water somewhat⁷). Hence, the reason for the high barrier for ions is not so much the electrostatic contribution of placing a charged particle at the center of an aqueous pore through a low dielectric membrane but the inability of water to wet (or solvate) the pore itself. Furthermore, in wider pores, which are readily filled by water, there exists considerable midrange ordering of the solvent induced by the ion, i.e., its hydration shell (radius of the second shell 0.53 nm), and by the wall (about two water layers, 0.6 nm).⁸ Combining these two ranges, we estimate that the solvent-mediated wall–ion interaction can extend to about

1 nm. Thus, ions will still be affected by the pore surface even if the pore is 10 times as wide as the bare ion.

Our simulations suggest that hydrophobic pores can pose high barriers to the permeation of ions, even when the pore radius is considerably larger than the ionic radius. The barrier originates in the high energetic cost for an ion to shed its first or, in wider pores, its second hydration shell. The barrier relates to the solvation energy for an ion/hydration shell complex in water. In the narrow selectivity filter of the potassium channels, evolution has demonstrated how to overcome dehydration barriers by solvating ions by carbonyl oxygens, which seamlessly replace water molecules in the first hydration shell,¹² leading to a vanishing barrier for ion permeation.²⁶ Evolution also seems to have exploited the barrier properties of hydrophobic pores in the control (gating) of ion channel activity.

Acknowledgment. We thank Nathan Baker, Graham Smith, and Marc Baaden for helpful discussions. This work was supported by The Wellcome Trust, BBSRC, and EPSRC.

Supporting Information Available: Computational details of the calculations, densities of water and Na^+ ions in a wide pore, PMFs for water, and a discussion of the influence of local flexibility of the pore wall (PDF). This material is available free of charge via the Internet at <http://pubs.acs.org>.

References

- (1) Gelb, L. D.; Gubbins, K. E.; Radhakrishnan, R.; Sliwinski-Bartkowiak, M. *Rep. Prog. Phys.* **1999**, *62*, 1573–1659.
- (2) Raviv, U.; Laurat, P.; Klein, J. *Nature* **2001**, *413*, 51–54.
- (3) Christenson, H. K. *J. Phys.: Condens. Matter* **2001**, *13*, R95–R133.
- (4) Koga, K.; Gao, G.; Tanaka, H.; Zeng, X. C. *Nature* **2001**, *412*, 802–805.
- (5) Hummer, G.; Rasaiah, J. C.; Noworyta, J. P. *Nature* **2001**, *414*, 188–190.
- (6) Levinger, N. E. *Science* **2002**, *298*, 1722–1723.
- (7) Beckstein, O.; Sansom, M. S. P. *Proc. Natl. Acad. Sci. U.S.A.* **2003**, *100*, 7063–7068.
- (8) Beckstein, O.; Sansom, M. S. P. *Physical Biology* **2004**, *1*, 42–52.
- (9) Baker, N. A.; Sept, D.; Joseph, S.; Holst, M. J.; McCammon, J. A. *Proc. Natl. Acad. Sci. U.S.A.* **2001**, *98*, 10037–10041.
- (10) Miyazawa, A.; Fujiyoshi, Y.; Unwin, N. *Nature* **2003**, *423*, 949–955.
- (11) Bass, R. B.; Strop, P.; Barclay, M.; Rees, D. C. *Science* **2002**, *298*, 1582–1587.
- (12) Zhou, Y.; Morais-Cabral, J. H.; Kaufman, A.; MacKinnon, R. *Nature* **2001**, *414*, 43–48.
- (13) Chang, G.; Spencer, R. H.; Lee, A. T.; Barclay, M. T.; Rees, D. C. *Science* **1998**, *282*, 2220–2226.
- (14) Parsegian, A. *Nature* **1969**, *221*, 844–846.
- (15) Rashin, A. A.; Honig, B. *J. Chem. Phys.* **1985**, *89*, 5588–5593.
- (16) Unwin, N. *J. Mol. Biol.* **1993**, *229*, 1101–1124.
- (17) Moe, P. C.; Levin, G.; Blount, P. *J. Biol. Chem.* **2000**, *275*, 31121–31127.
- (18) Beckstein, O.; Biggin, P. C.; Sansom, M. S. P. *J. Phys. Chem. B* **2001**, *105*, 12902–12905.
- (19) Kirkwood, J. G. *J. Chem. Phys.* **1935**, *3*, 300–313.
- (20) Roux, B.; Allen, T.; Bernèche, S.; Im, W. *Quart. Rev. Biophys.* **2004**, *37*, 15–103.
- (21) Lindahl, E.; Hess, B.; van der Spoel, D. *J. Mol. Mod.* **2001**, *7*, 306–317.
- (22) Valleau, J. P.; Torrie, G. M. A Guide to Monte Carlo for Statistical Mechanics: 2. Byways. In *Statistical Mechanics. Part A: Equilibrium Techniques*; Berne, B. J., Ed.; Plenum Press: New York, 1977; Vol. 5.
- (23) Kumar, S.; Bouzida, D.; Swendsen, R. H.; Kollman, P. A.; Rosenberg, J. M. *J. Comput. Chem.* **1992**, *13*, 1011–1021.
- (24) Edwards, S.; Corry, B.; Kuyucak, S.; Chung, S.-H. *Biophys. J.* **2002**, *83*, 1348–1360.
- (25) Allen, T. W.; Andersen, O. S.; Roux, B. *Proc. Natl. Acad. Sci. U.S.A.* **2004**, *101*, 117–122.
- (26) Bernèche, S.; Roux, B. *Nature* **2001**, *414*, 73–77.

JA045271E